LONG-LIVED LIGHT SCALARS AT THE LHC*

P.S. Bhupal Dev

Department of Physics and McDonnell Center for the Space Sciences
Washington University, St. Louis, MO 63130, USA

Rabindra N. Mohapatra

Maryland Center for Fundamental Physics, Department of Physics
University of Maryland, College Park, MD 20742, USA

Yongchao Zhang

Service de Physique Théorique, Université Libre de Bruxelles
Boulevard du Triomphe, CP225, 1050 Brussels, Belgium

(Received March 31, 2017)

In the minimal left–right realization of TeV scale seesaw for neutrino masses, there is a phenomenologically allowed range of parameters where one of the neutral scalar particles from the right-handed symmetry breaking sector could have a mass at the GeV scale. We discuss the constraints on this particle from low-energy flavor observables, and find that such a light particle is necessarily long-lived, and can be searched for at the LHC via displaced signals of a collimated photon jet. This decay mode provides a new test of TeV scale left–right seesaw model since this is in sharp contrast with any generic beyond the Standard Model light scalar, which would decay to leptons and jets as well.

DOI:10.5506/APhysPolB.48.969

1. Introduction

The discovery of neutrino masses has provided the first laboratory evidence for physics beyond the Standard Model (BSM). The nature of the underlying new physics is however unclear and a "leave no stone unturned" approach is called for to pinpoint this, since the result would have a profound impact on the ongoing new physics searches by narrowing the vast

* Presented by P.S.B. Dev at the Cracow Epiphany Conference "Particle Theory Meets the First Data from LHC Run2", Kraków, Poland, January 9–12, 2017.

BSM landscape. We explore this question using the seesaw paradigm which is a simple and well-motivated way to understand neutrino masses [1–5], and considering its ultraviolet-complete realization within a TeV-scale left–right symmetric model (LRSM) framework [6–8], based on the gauge group $\mathcal{G}_{\rm LR} \equiv {\rm SU}(2)_{\rm L} \times {\rm SU}(2)_{\rm R} \times {\rm U}(1)_{B-L}$. The experimental signals of this model have been extensively studied in the literature and have generally involved the heavy gauge bosons and heavy right-handed neutrinos (RHNs) [9–20] or heavy Higgs bosons [21–26].

In these proceedings, we point out a new probe of this model by focussing on the CP-even remnant of the predominantly ${\rm SU}(2)_{\rm R}$-triplet Higgs field (H_3) that breaks the ${\rm SU}(2)_{\rm R} \times {\rm U}(1)_{B-L}$ gauge symmetry of the model. It is the analog of the SM Higgs field (h) for the seesaw extension. For a TeV seesaw scale, its mass can be anywhere from a GeV to TeV. The decay and production properties of H_3 when its mass is much higher than the SM Higgs mass was studied in Refs. [24, 27, 28]. The mass range close to m_h is disfavored by the current LHC Higgs data, barring fine tuning of parameters to suppress the h–H_3 mixing. However, the mass range $m_{H_3} \ll m_h$ was overlooked in the literature, and this is the subject of these proceedings, which are based on Refs. [29, 30].

2. Light neutral scalar

The minimal LRSM consists of the following Higgs fields:

$$\Phi = \begin{pmatrix} \phi_1^0 & \phi_2^+ \\ \phi_1^- & \phi_2^0 \end{pmatrix}, \qquad \Delta_{\rm R} = \begin{pmatrix} \Delta_{\rm R}^+/\sqrt{2} & \Delta_{\rm R}^{++} \\ \Delta_{\rm R}^0 & -\Delta_{\rm R}^+/\sqrt{2} \end{pmatrix}, \tag{1}$$

which transform under $\mathcal{G}_{\rm LR}$ as ($\mathbf{2}$, $\mathbf{2}$, 0) and ($\mathbf{1}$, $\mathbf{3}$, 2), respectively. The group $\mathcal{G}_{\rm LR}$ is broken down to the EW gauge group by the triplet vacuum expectation value (VEV) $\langle \Delta_{\rm R}^0 \rangle = v_{\rm R}$, whereas the EW symmetry is broken by the bidoublet VEV $\langle \Phi \rangle = {\rm diag}(\kappa, \kappa')$, with the EW VEV $v_{\rm EW} = \sqrt{\kappa^2 + \kappa'^2}$. For simplicity, we assume that the discrete parity symmetry has been broken at a scale much larger than the ${\rm SU}(2)_{\rm R}$-breaking scale [31], but our conclusions remain unchanged in the TeV-scale fully parity-symmetric version of the LRSM.

The most general scalar potential involving Φ and $\Delta_{\rm R}$ is

$$\begin{aligned}\mathcal{V} = & -\mu_1^2\,{\rm Tr}\left(\Phi^\dagger\Phi\right) - \mu_2^2\left[{\rm Tr}\left(\tilde\Phi\Phi^\dagger\right) + {\rm Tr}\left(\tilde\Phi^\dagger\Phi\right)\right] - \mu_3^2{\rm Tr}\left(\Delta_{\rm R}\Delta_{\rm R}^\dagger\right) \\ & +\lambda_1\left[{\rm Tr}\left(\Phi^\dagger\Phi\right)\right]^2 + \lambda_2\left\{\left[{\rm Tr}\left(\tilde\Phi\Phi^\dagger\right)\right]^2 + \left[{\rm Tr}\left(\tilde\Phi^\dagger\Phi\right)\right]^2\right\} \\ & +\lambda_3\,{\rm Tr}\left(\tilde\Phi\Phi^\dagger\right){\rm Tr}\left(\tilde\Phi^\dagger\Phi\right) + \lambda_4{\rm Tr}\left(\Phi^\dagger\Phi\right)\left[{\rm Tr}\left(\tilde\Phi\Phi^\dagger\right) + {\rm Tr}\left(\tilde\Phi^\dagger\Phi\right)\right]\end{aligned}$$

$$
\begin{aligned}
&+\rho_1 \left[\mathrm{Tr}\left(\Delta_{\mathrm{R}}\Delta_{\mathrm{R}}^{\dagger}\right)\right]^2 + \rho_2\,\mathrm{Tr}\left(\Delta_{\mathrm{R}}\Delta_{\mathrm{R}}\right)\mathrm{Tr}\left(\Delta_{\mathrm{R}}^{\dagger}\Delta_{\mathrm{R}}^{\dagger}\right)\\
&+\alpha_1\,\mathrm{Tr}\left(\Phi^{\dagger}\Phi\right)\mathrm{Tr}\left(\Delta_{\mathrm{R}}\Delta_{\mathrm{R}}^{\dagger}\right) + \left[\alpha_2 e^{i\delta_2}\mathrm{Tr}\left(\tilde{\Phi}^{\dagger}\Phi\right)\mathrm{Tr}\left(\Delta_{\mathrm{R}}\Delta_{\mathrm{R}}^{\dagger}\right) + \mathrm{H.c.}\right]\\
&+\alpha_3\,\mathrm{Tr}\left(\Phi^{\dagger}\Phi\Delta_{\mathrm{R}}\Delta_{\mathrm{R}}^{\dagger}\right)\,. \qquad (2)
\end{aligned}
$$

One physical scalar from the bidoublet is identified as the SM Higgs h, while the other 4 degrees from the heavy doublet $(H_1, A_1, H_1^{\pm})$ have nearly degenerate mass, which is constrained to be $\gtrsim 10$ TeV from FCNC constraints [32, 33]. Similarly, the mass of the doubly-charged scalars $H_2^{\pm\pm}$ from Δ_{R} is required to be above a few hundred GeV from same-sign dilepton pair searches at the LHC [25, 26]. However, no constraint was available in the literature for the remaining neutral scalar field H_3, consisting predominantly of the real component of Δ_{R}^0, mainly due to the fact that it has no direct couplings to the SM sector and couples only to the heavy gauge bosons W_{R}, Z_{R} and the RHNs, in the limit of no mixing with other scalars. Therefore, its tree-level mass could, in principle, be much lower than the v_{R} scale, as long as the quartic coupling $\rho_1 \ll 1$. This makes it the only possible light scalar in the model, and due to its suppressed couplings to the SM sector, it is also a natural LLP candidate at the LHC and in future colliders.

Since we envision that H_3 mass is much less than the v_{R} scale, it is important to consider the loop corrections and see whether this small mass is radiatively stable. Recall that in the SM, if we neglect the one-loop fermion contributions to the Coleman–Weinberg effective potential [34], there is a lower limit of the order of 5 GeV on the Higgs boson mass [35]. This bound goes away once the top-quark Yukawa coupling is included. Similarly, it was pointed out in Ref. [36] that in a class of LRSM, there is a lower bound of about 900 GeV on the real part of the doublet scalar field coming from purely gauge contributions. Inclusion of the Yukawa interactions to the RHNs in the minimal LRSM we are considering allows us to avoid this bound and have a very light H_3.

Quantitatively, keeping only the Δ_{R}^0 terms in the one-loop effective potential, we obtain the correction term

$$
\frac{3}{2\pi^2}\left[\frac{1}{3}\alpha_3^2 + \frac{8}{3}\rho_2^2 - 8f^4 + \frac{1}{2}g_{\mathrm{R}}^4 + \left(g_{\mathrm{R}}^2 + g_{BL}^2\right)^2\right] v_{\mathrm{R}}^2\,, \qquad (3)
$$

where g_{R} and g_{BL} are respectively the $\mathrm{SU}(2)_{\mathrm{R}}$ and $\mathrm{U}(1)_{B-L}$ gauge coupling strengths. We have assumed the three RHNs in the LRSM to be approximately degenerate with the same Yukawa coupling f. From Eq. (3), one would naïvely expect the loop correction to be of the order of $v_{\mathrm{R}}/4\pi$. However, the gauge and fermion contributions can cancel each other; with a mild tuning of g_{R} and f at the level of $\mathrm{GeV}/v_{\mathrm{EW}} \simeq 10^{-2}$, we can easily obtain a loop correction at or below the GeV scale. It is remarkable to note that the TeV scale seesaw prefers the natural value for Majorana–Yukawa couplings to be of the order of one, implying in turn TeV scale RHNs with observable same-sign dilepton plus dijet signatures at the LHC.

3. Couplings and decay

When the mass of H_3 is well below the EW scale, it decays to the light SM fermions through mixing with the SM Higgs h and the heavy CP-even scalar H_1 from Φ, with the mixing angles respectively given by

$$\sin\theta_1 \simeq \frac{\alpha_1}{2\lambda_1}\frac{v_{\rm R}}{v_{\rm EW}}\,, \qquad \sin\theta_2 \simeq \frac{4\alpha_2}{\alpha_3}\frac{v_{\rm EW}}{v_{\rm R}}\,. \tag{4}$$

Note the inverted dependence on the VEV ratio $(v_{\rm EW}/v_{\rm R})^{-1}$ for the h–H_3 mixing, because the SM Higgs boson mass is of the order of $v_{\rm EW}$. The quartic couplings $\alpha_{1,2}$ connect H_3 to h and H_1 respectively, and are usually suppressed by higher powers of $v_{\rm EW}/v_{\rm R}$. There is an alignment limit of the parameter space for $\alpha_{1,2} \to 0$, when H_3 is secluded from mixing with other scalars in the LRSM, and λ_1 approaches to $\lambda_{\rm SM} = m_h^2/4v_{\rm EW}^2$. Thus for TeV-scale $v_{\rm R}$, both the mixing angles $\sin\theta_{1,2}$ are naturally small.

At the one-loop level, the gauge and Yukawa couplings induce the decay of H_3 into digluons and diphotons, as in the SM Higgs case. However, when the FCNC constraints on the mixing angles $\sin\theta_{1,2}$ are considered (see below), the diphoton channel is dominated by the $W_{\rm R}$ loop which is suppressed only by the RH scale $v_{\rm R}$: $\Gamma_{\gamma\gamma} \propto v_{\rm R}^{-2}$. The heavy charged scalar loops ($H_1^\pm$ and $H_2^{\pm\pm}$) are subleading. The SM W loop is heavily suppressed by the W–$W_{\rm R}$ mixing. All the couplings and partial decay widths of H_3 can be found in Refs. [29, 30].

Contours of fixed decay length L_0 of H_3 *at rest* are shown in the m_{H_3}–$\sin\theta_1$ plane of Fig. 1 (dashed grey lines). For concreteness, we have made the following reasonable assumptions: *(i)* The RH scale $v_{\rm R} = 5$ TeV, which is the smallest value required to satisfy the current LHC limits on $W_{\rm R}$ mass. We also set the H_3–H_1 mixing $\sin\theta_2 = 0$. *(ii)* In the minimal LRSM, the RH quark mixing $V_{\rm R}$ is very similar to the CKM matrix $V_{\rm L}$, up to some additional phases. For simplicity, we adopt $V_{\rm R} = V_{\rm L}$ in the calculation. *(iii)* The couplings to charged leptons depend on the heavy- and light-neutrino sector via the Yukawa coupling matrix $Y_{\nu N}$. Here, we assume the light neutrinos are of normal hierarchy with the lightest neutrino mass of 0.01 eV and the three RHNs degenerate at 1 TeV without any RH lepton mixing, which pushes the couplings $Y_{\nu N} \sim 10^{-7}$. Furthermore, the flavor-changing decay modes are included, such as $H_3 \to sb, \mu\tau$, and the running of strong coupling $\alpha_{\rm s}$ is taken into consideration, which is important below the EW scale.

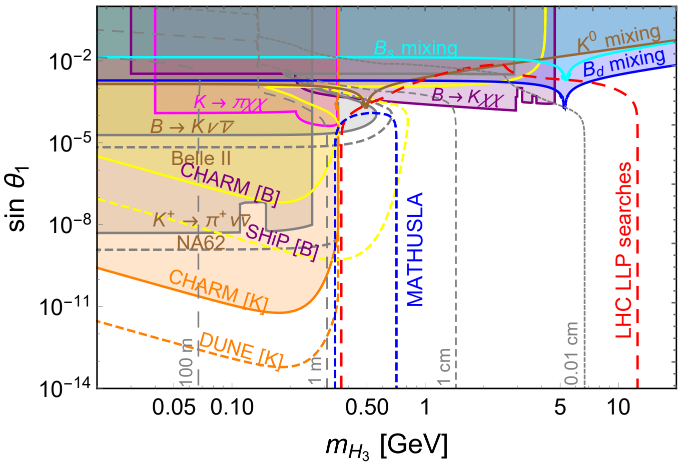

Fig. 1. (Color online) Contours of H_3 decay length at rest (dashed gray lines) as functions of its mass and mixing with the SM Higgs boson. Superimposed are limits (shaded/color) from meson mixing (K^0, $B_{d,s}$) and rare meson decays $K \to \pi\chi\chi$, $B \to K\chi\chi$ ($\chi = e, \mu, \gamma$), $K \to \pi\nu\bar{\nu}$, $B \to K\nu\bar{\nu}$ and $K \to \pi H_3 \to \pi\gamma\gamma$ and $B \to K H_3 \to K\gamma\gamma$ at beam-dump experiments. Also shown are the projected sensitivities from LLP searches at the LHC and MATHUSLA.

From the lifetime curves in Fig. 1, it is clear that when m_{H_3} is below a few GeV, it tends to be long-lived, with decay lengths $L \gtrsim 0.01\,b$ cm (where $b = E_{H_3}/m_{H_3}$ is the Lorentz boost factor, whose distribution typically peaks at around 100 for a GeV-scale particle produced at the LHC energy), as long as the mixing angles $\sin\theta_{1,2}$ are small $\lesssim 10^{-4}$, which is guaranteed by the flavor constraints, as discussed below. With the couplings to fermions constrained by the flavor data, only the diphoton channel is significant, implying that H_3 decays mostly into two displaced photons at the LHC.

4. Low-energy flavor constraints

Due to its mixing with the SM Higgs h, as well as the heavy scalar H_1, the light scalar H_3 has induced flavor-changing couplings to the SM quarks, which are severely constrained by the low-energy flavor data, *e.g.* from K–$\bar{K}$, B_d–$\bar{B}_d$ and B_s–$\bar{B}_s$ neutral meson mixing, as well as rare K and B meson decays to lighter mesons and a photon pair. Although the couplings originate from the FCNC couplings of H_1, as the masses of H_1 and H_3 are independent observables, the flavor constraints on H_3 derived below are different from those on the heavy scalar H_1.

Taking the K^0–$\bar{K}^0$ mixing as an explicit example, we cast the flavor-changing four-fermion interactions mediated by H_3 into a linear combination of the effective dimension-6 operators of the form of

$$\mathcal{O} = \mu_{\rm RL}^2 \mathcal{O}_2 + \mu_{\rm LR}^2 \tilde{\mathcal{O}}_2 + 2\mu_{\rm RL}\mu_{\rm LR}\, \mathcal{O}_4\,, \tag{5}$$

where $\mu_{\rm RL,\,LR} = \sum_i m_i \lambda_i^{\rm RL,\,LR}$ with $m_i = \{m_u, m_c, m_t\}$ the running up-type quark masses, $\lambda_i^{\rm LR} = V_{{\rm L},\,i2}^* V_{{\rm R},\,i1}$ and $\lambda_i^{\rm RL} = V_{{\rm R},\,i2}^* V_{{\rm L},\,i1}$ the left- and right-handed quark mixing matrix elements, and

$$\begin{aligned} \mathcal{O}_2 &= [\bar{s}(1-\gamma_5)d]\,[\bar{s}(1-\gamma_5)d]\,, \\ \tilde{\mathcal{O}}_2 &= [\bar{s}(1+\gamma_5)d]\,[\bar{s}(1+\gamma_5)d]\,, \\ \mathcal{O}_4 &= [\bar{s}(1-\gamma_5)d]\,[\bar{s}(1+\gamma_5)d] \end{aligned} \tag{6}$$

with $P_{\rm L,R} = \frac{1}{2}(1 \mp \gamma_5)$. The effective Lagrangian we need is thus given by

$$\mathcal{L}_{H_3}^K = \frac{G_{\rm F}}{\sqrt{2}} \frac{\sin^2\tilde{\theta}_2}{m_K^2 - m_{H_3}^2 + i m_{H_3} \mathit{\Gamma}_{H_3}} \mathcal{O}\,, \tag{7}$$

where $G_{\rm F}$ is the Fermi constant and $\sin\tilde{\theta}_2 = \sin\theta_2 + \xi\sin\theta_1$ is the "effective" mixing angle, which also involves the mixing with the SM Higgs, as h mixes with H_1 with a small angle $\xi \simeq m_b/m_t$. Although the flavor-changing couplings of H_3 arise from its mixing with H_1, the effective Lagrangian (7) is not simply multiplied by a factor of $\sin\tilde{\theta}_2$; in particular, the operators of the form of $\mathcal{O}_2$ and $\tilde{\mathcal{O}}_2$ are absent in the H_1 case, which are canceled by the CP-odd scalar A_1 in the mass degenerate limit of $m_{H_1} = m_{A_1}$. In Eq. (5), the charm-quark contribution $m_c\lambda$ dominates (λ being the Cabibbo angle), with a subleading contribution $\sim m_t\lambda^5$ from the top quark.

Requiring that the light H_3-mediated contribution be consistent with the current data on Δm_K, *i.e.* $< 1.74 \times 10^{-12}$ MeV [38], leads to an upper limit on the mixing angles $\sin\theta_{1,2}$, as presented in Fig. 1 (solid/red line) for θ_1 (the limit on θ_2 is stronger by a factor of m_t/m_b). As expected from the propagator structure in Eq. (7), the limits on the mixing angles $\sin\theta_{1,2}$ are significantly strengthened in the narrow resonance region, where $m_{H_3} \simeq m_K$. For $m_{H_3} \ll m_K$, the H_3 propagator is dominated by the momentum term

$$\frac{1}{q^2 - M_{H_3}^2 + i M_{H_3} \mathit{\Gamma}_{H_3}} \to \frac{1}{q^2} \simeq \frac{1}{m_K^2}\,, \tag{8}$$

and the limit approaches to a constant value, whereas for $m_{H_3} \gg m_K$, the limit scales as $m_{H_3}^{1/2}$.

The calculation of flavor constraints from B_d and B_s mixing is quite similar to those from K^0 [30]. Unlike the K^0 case, the top-quark contribution dominates the effective coupling $\sum_i m_i \lambda_i^{\rm LR,\,RL}$ and strengthens the corresponding limits on the couplings of H_3 to the bottom quark. The mixing limits from $\Delta m_{B_d} < 9.3 \times 10^{-11}$ MeV and $\Delta m_{B_s} < 2.7 \times 10^{-9}$ MeV are shown in Fig. 1, respectively, as the solid blue and cyan lines. The B mesons are 10 times heavier than the K meson, and the absolute values of error bars for Δm_B are much larger than that for Δm_K; this makes the B-mixing limits weaker than K-mixing limit for $m_{H_3} \ll m_B$. However, this could be partially compensated by the large effective coupling $\sum_i m_i \lambda_i^{\rm LR}$ when H_3 is heavier. Thus, for $m_{H_3} \gtrsim 1$ GeV, the limits on $\sin\theta_{1,2}$ from the B_d mixing turn out to be more stringent.

A light H_3 could also be produced in rare meson decays via the flavor-changing couplings, if kinematically allowed. The corresponding SM decay modes are either forbidden or highly suppressed by loop factors and the CKM matrix elements; thus, these rare decay channels are also expected to set stringent limits on $\sin\theta_{1,2}$. We consider the decays $B \to KH_3$ and $K \to \pi H_3$ each followed by $H_3 \to \chi\chi$, with $\chi = e^+e^-, \mu^+\mu^-, \gamma\gamma$. The rare SM processes $K \to \pi\chi\chi$ and $B \to K\chi\chi$ have been searched for in NA48/2 [39, 40], NA62 [41], KTeV [42–45], BaBar [46], Belle [47], LHCb [48]. All the high intensity meson decay experiments are listed in Table I, and the limits on the mixing angle $\sin\theta_1$ are collectively depicted in Fig. 1, where, conservatively, we demand H_3 decays inside the detector partial resolution $L_{H_3} < 0.1$ mm, and the branching ratios $\mathrm{BR}(H_3 \to \chi\chi)$ and Lorentz boost factor E_{H_3}/m_{H_3} from meson decay have been taken into consideration[1]. More details can be found in Refs. [29, 30].

After being produced from meson decay, if H_3 decays outside the detector, the signal is $d_j \to d_i$ at the parton level plus missing energy. This could be constrained by the current limits of $K \to \pi\nu\bar{\nu}$ from E949 [50–53] and $B \to K\nu\bar{\nu}$ from BaBar [54], and future prospects at NA62 [55] and Belle II [56], which are all presented in Fig. 1. As light H_3 tends to be long-lived, the "invisible" searches with neutrinos in the final state are more constraining than "visible" decay modes above. With a huge number of protons-on-target and rather long decay length, the beam-dump experiments could further improve the limits. The current limits from CHARM [57] and future prospects at SHiP [58] and DUNE [59] are also shown in Fig. 1, which could exclude the mixing angle up to the level of 10^{-13}.

Note that the mixing angle $\sin\theta_1$ could also be constrained by the precise Higgs measurements, invisible SM Higgs decay, rare decays $Z \to \gamma H_3$ and $t \to uH_3, cH_3$. However, these limits are much weaker than those from meson oscillation and decay, at most of the order of 0.1, and are not shown here.

---

[1] On the cosmological side, when H_3 mass is below $\sim$50 MeV, it will start contributing to dark radiation as $\Delta N_{\rm eff} \simeq 4/7$, which is ruled out by the Planck data [49] at the 2.5σ C.L. Therefore, we will consider only H_3 with mass $\gtrsim 50$ MeV in the following.

TABLE I

Summary of meson decay constraints used to derive current/future limits in Fig. 1. The last column gives the upper limit on the BR (number of events $N_{\rm event}$) of the corresponding process. More details can be found in Refs. [29, 30].

Expt.	Meson decay	H_3 decay	E_{H_3}	L_{H_3}	BR ($N_{\rm event}$)
NA48/2	$K^+ \to \pi^+ H_3$	$H_3 \to e^+e^-$	~ 30 GeV	< 0.1 mm	2.63×10^{-7}
NA48/2	$K^+ \to \pi^+ H_3$	$H_3 \to \mu^+\mu^-$	~ 30 GeV	< 0.1 mm	8.88×10^{-8}
NA62	$K^+ \to \pi^+ H_3$	$H_3 \to \gamma\gamma$	~ 37 GeV	< 0.1 mm	4.70×10^{-7}
E949	$K^+ \to \pi^+ H_3$	any (inv.)	~ 355 MeV	> 4 m	4×10^{-10}
NA62	$K^+ \to \pi^+ H_3$	any (inv.)	~ 37.5 GeV	> 2 m	2.4×10^{-11}
KTeV	$K_{\rm L} \to \pi^0 H_3$	$H_3 \to e^+e^-$	~ 30 GeV	< 0.1 mm	2.8×10^{-10}
KTeV	$K_{\rm L} \to \pi^0 H_3$	$H_3 \to \mu^+\mu^-$	~ 30 GeV	< 0.1 mm	4×10^{-10}
KTeV	$K_{\rm L} \to \pi^0 H_3$	$H_3 \to \gamma\gamma$	~ 40 GeV	< 0.1 mm	3.71×10^{-7}
BaBar	$B \to K H_3$	$H_3 \to \ell^+\ell^-$	$\sim m_B/2$	< 0.1 mm	7.91×10^{-7}
Belle	$B \to K H_3$	$H_3 \to \ell^+\ell^-$	$\sim m_B/2$	< 0.1 mm	4.87×10^{-7}
LHCb	$B^+ \to K^+ H_3$	$H_3 \to \mu^+\mu^-$	~ 150 GeV	< 0.1 mm	4.61×10^{-7}
BaBar	$B \to K H_3$	any (inv.)	$\sim m_B/2$	> 3.5 m	3.2×10^{-5}
Belle II	$B \to K H_3$	any (inv.)	$\sim m_B/2$	> 3 m	4.1×10^{-6}
CHARM	$K \to \pi H_3$	$H_3 \to \gamma\gamma$	~ 10 GeV	[480, 515] m	(< 2.3)
CHARM	$B \to X_s H_3$	$H_3 \to \gamma\gamma$	~ 10 GeV	[480, 515] m	(< 2.3)
SHiP	$B \to X_s H_3$	$H_3 \to \gamma\gamma$	~ 25 GeV	[70, 125] m	(< 3)
DUNE	$K \to \pi H_3$	$H_3 \to \gamma\gamma$	~ 12 GeV	[500, 507] m	(< 3)

5. Displaced diphoton signal at the LHC

For a GeV-scale H_3, the h–H_3 mixing is so severely constrained that its Higgs portal production is suppressed and it could only be produced via the gauge coupling through heavy vector boson fusion (VBF): $pp \to W_{\rm R}^* W_{\rm R}^* jj \to H_3 jj$, with a subleading contribution from $Z_{\rm R}$ fusion [24]. The associated production of $W_{\rm R} H_3$ is further suppressed by the heavy gauge boson mass in the final state. When $m_{H_3} \lesssim 10$ GeV, the VBF production rate is almost constant for a given $v_{\rm R}$, and is sensitive only to the gauge coupling $g_{\rm R}$. For a smaller $g_{\rm R} < g_{\rm L}$, the $W_{\rm R}$ boson is lighter and the production of H_3 can be significantly enhanced. For three benchmark values of $g_{\rm R}/g_{\rm L} = 0.6$, 1 and 1.5, the leading order production cross sections at $\sqrt{s} = 14$ TeV are, respectively, 0.10 fb, 1.1 fb and 4.9 fb, when we apply the cuts $p_{\rm T}(j) > 25$ GeV and $\Delta\phi(jj) > 0.4$ on the jets and set $v_{\rm R} = 5$ TeV.

Limited by the flavor data, a light H_3 decays mostly into the diphoton final state at the LHC after being produced. For a GeV mass, the decay-at-rest length L_0 is of the order of cm; multiplied by a boost factor of $b \sim 100$, the actual decay length is expected to be of the order of m, comparable to the radius of the Electromagnetic Calorimeter (ECAL) of ATLAS and CMS detectors, which are respectively 1.5 m [60] and 1.3 m [61]. The final-state photons from H_3 decay are highly collimated with a separation of $\Delta R \sim m_{H_3}/E_{H_3}$. Thus, most of the photon pairs cannot be separated with the angular resolution of $\Delta\eta \times \Delta\phi = 0.025 \times 0.025$ (ATLAS) and 0.0174×0.0174 (CMS) [60, 61], and would be identified as a high-energy single-photon jet. Counting conservatively these single photon jets within $1\,\mathrm{cm} < L < R_{\mathrm{ECAL}}$, we can have up to thousands of signal events for an integrated luminosity of 3000 fb^{-1} at $\sqrt{s} = 14$ TeV LHC, depending on the RH scale v_{R} and gauge coupling g_{R}. The SM fake rate for the displaced diphotons is expected to be small, thus the displaced photon events (with the associated VBF jets) would constitute a new "smoking gun" signature of the H_3 decays as predicted by the minimal LRSM. For $m_{H_3} \lesssim 1$ GeV, the decay length exceeds the size of the LHC detectors, but could be just suitable for future dedicated LLP search experiments, such as MATHUSLA [62], as shown in Fig. 1.

The projected probable regions in the plane of m_{H_3} and $m_{W_{\mathrm{R}}}$ are presented in Fig. 2, for three benchmark values of $g_{\mathrm{R}}/g_{\mathrm{L}} = 0.6$, 1 and 1.5, where we have assumed 10 and 4 signal events of displaced photon jets at respectively the LHC and MATHUSLA. This is largely complementary to the direct searches of W_{R} via same-sign dilepton plus jets, and could reveal directly the TeV-scale seesaw mechanism at the high-energy frontier. The LLP searches at the LHC are sensitive to larger values of the light

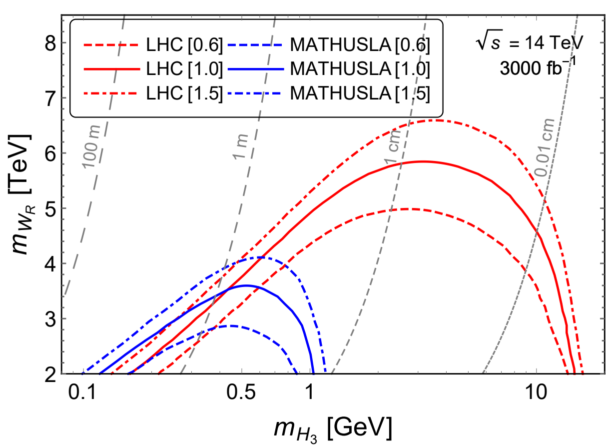

Fig. 2. Sensitivity contours in the m_{H_3}–$m_{W_{\mathrm{R}}}$ plane from LLP searches at the LHC and MATHUSLA, for $g_{\mathrm{R}}/g_{\mathrm{L}} = 0.6$, 1 and 1.5. The gray contours indicate the proper lifetime of H_3 with $g_{\mathrm{R}} = g_{\mathrm{L}}$; for $g_{\mathrm{R}} \neq g_{\mathrm{L}}$, the lifetime has to be rescaled by the factor of $(g_{\mathrm{R}}/g_{\mathrm{L}})^{-2}$.

scalar mass, as compared to the low-energy meson decay searches, due to large Lorentz boost factors, and are, therefore, complementary to the meson probes at the high-intensity frontier. Moreover, the dominant diphoton decay channel of the light scalar considered here is a unique feature of the LRSM that can be used to distinguish it from other beyond SM scenarios.

6. Summary

We have pointed out that searches for light neutral scalars via high energy displaced photon searches at the LHC could provide a new probe of the TeV scale left–right seesaw models. We have derived the low-energy flavor constraints on such particles, and have given the predictions for the displaced photon signal from its production and decay at the LHC. The searches of displaced photon signal at the high-energy frontier, *i.e.* the LHC and future 100 TeV hadron colliders, are largely complementary to the rare meson decay at the high-intensity frontier, such as the SHiP and DUNE experiments.

P.S.B.D. would like to thank the organizers of the XXIII Cracow Epiphany Conference for the invitation to present this work. The work of R.N.M. is supported by the U.S. National Science Foundation grant No. PHY1620074. Y.Z. would like to thank the IISN and Belgian Science Policy (IAP VII/37) for support.

REFERENCES

[1] P. Minkowski, *Phys. Lett. B* **67**, 421 (1977).
[2] R.N. Mohapatra, G. Senjanović, *Phys. Rev. Lett.* **44**, 912 (1980).
[3] T. Yanagida, *Conf. Proc. C* **7902131**, 95 (1979).
[4] M. Gell-Mann, P. Ramond, R. Slansky, *Conf. Proc. C* **790927**, 315 (1979) [arXiv:1306.4669 [hep-th]].
[5] S.L. Glashow, *NATO Sci. Ser. B* **61**, 687 (1980).
[6] J.C. Pati, A. Salam, *Phys. Rev. D* **10**, 275 (1974).
[7] R.N. Mohapatra, J.C. Pati, *Phys. Rev. D* **11**, 2558 (1975).
[8] G. Senjanović, R.N. Mohapatra, *Phys. Rev. D* **12**, 1502 (1975).
[9] W.Y. Keung, G. Senjanović, *Phys. Rev. Lett.* **50**, 1427 (1983).
[10] A. Ferrari *et al.*, *Phys. Rev. D* **62**, 013001 (2000).
[11] M. Nemevsek, F. Nesti, G. Senjanović, Y. Zhang, *Phys. Rev. D* **83**, 115014 (2011) [arXiv:1103.1627 [hep-ph]].
[12] S.P. Das, F.F. Deppisch, O. Kittel, J.W.F. Valle, *Phys. Rev. D* **86**, 055006 (2012) [arXiv:1206.0256 [hep-ph]].
[13] C.Y. Chen, P.S.B. Dev, R.N. Mohapatra, *Phys. Rev. D* **88**, 033014 (2013) [arXiv:1306.2342 [hep-ph]].

[14] F.F. Deppisch, P.S.B. Dev, A. Pilaftsis, *New J. Phys.* **17**, 075019 (2015) [arXiv:1502.06541 [hep-ph]].
[15] J. Gluza, T. Jeliński, *Phys. Lett. B* **748**, 125 (2015) [arXiv:1504.05568 [hep-ph]].
[16] P.S.B. Dev, D. Kim, R.N. Mohapatra, *J. High Energy Phys.* **1601**, 118 (2016) [arXiv:1510.04328 [hep-ph]].
[17] M. Lindner, F.S. Queiroz, W. Rodejohann, C.E. Yaguna, *J. High Energy Phys.* **1606**, 140 (2016) [arXiv:1604.08596 [hep-ph]].
[18] R. Ruiz, arXiv:1703.04669 [hep-ph].
[19] V. Khachatryan *et al.* [CMS Collaboration], *Eur. Phys. J. C* **74**, 3149 (2014) [arXiv:1407.3683 [hep-ex]].
[20] G. Aad *et al.* [ATLAS Collaboration], *J. High Energy Phys.* **1507**, 162 (2015) [arXiv:1506.06020 [hep-ex]].
[21] J.F. Gunion *et al.*, PRINT-86-1324 (UC, DAVIS).
[22] G. Azuelos, K. Benslama, J. Ferland, *J. Phys. G* **32**, 73 (2006) [arXiv:hep-ph/0503096].
[23] G. Bambhaniya *et al.*, *Phys. Rev. D* **92**, 015016 (2015) [arXiv:1504.03999 [hep-ph]].
[24] P.S.B. Dev, R.N. Mohapatra, Y. Zhang, *J. High Energy Phys.* **1605**, 174 (2016) [arXiv:1602.05947 [hep-ph]].
[25] ATLAS Collaboration, ATLAS-CONF-2016-051.
[26] CMS Collaboration, CMS-PAS-HIG-16-036.
[27] A. Maiezza, M. Nemevsek, F. Nesti, *Phys. Rev. Lett.* **115**, 081802 (2015) [arXiv:1503.06834 [hep-ph]].
[28] M. Nemevsek, F. Nesti, J.C. Vasquez, *J. High Energy Phys.* **1704**, 114 (2017) [arXiv:1612.06840 [hep-ph]].
[29] P.S.B. Dev, R.N. Mohapatra, Y. Zhang, arXiv:1612.09587 [hep-ph].
[30] P.S.B. Dev, R.N. Mohapatra, Y. Zhang, arXiv:1703.02471 [hep-ph].
[31] D. Chang, R.N. Mohapatra, M.K. Parida, *Phys. Rev. Lett.* **52**, 1072 (1984).
[32] Y. Zhang, H. An, X. Ji, R.N. Mohapatra, *Nucl. Phys. B* **802**, 247 (2008) [arXiv:0712.4218 [hep-ph]].
[33] S. Bertolini, A. Maiezza, F. Nesti, *Phys. Rev. D* **89**, 095028 (2014) [arXiv:1403.7112 [hep-ph]].
[34] S. Coleman, E. Weinberg, *Phys. Rev. D* **7**, 1888 (1973).
[35] A.D. Linde, *JETP Lett.* **23**, 64 (1976); S. Weinberg, *Phys. Rev. Lett.* **36**, 294 (1976).
[36] M. Holthausen, M. Lindner, M.A. Schmidt, *Phys. Rev. D* **82**, 055002 (2010) [arXiv:0911.0710 [hep-ph]].
[37] R. Babich *et al.*, *Phys. Rev. D* **74**, 073009 (2006) [arXiv:hep-lat/0605016].
[38] C. Patrignani *et al.* [Particle Data Group], *Chin. Phys. C* **40**, 100001 (2016).
[39] J.R. Batley *et al.* [NA48/2 Collaboration], *Phys. Lett. B* **677**, 246 (2009) [arXiv:0903.3130 [hep-ex]].

[40] J.R. Batley *et al.* [NA48/2 Collaboration], *Phys. Lett. B* **697**, 107 (2011) [arXiv:1011.4817 [hep-ex]].
[41] C. Lazzeroni *et al.* [NA62 Collaboration], *Phys. Lett. B* **732**, 65 (2014) [arXiv:1402.4334 [hep-ex]].
[42] A. Alavi-Harati *et al.* [KTeV Collaboration], *Phys. Rev. Lett.* **93**, 021805 (2004) [arXiv:hep-ex/0309072].
[43] A. Alavi-Harati *et al.* [KTEV Collaboration], *Phys. Rev. Lett.* **84**, 5279 (2000) [arXiv:hep-ex/0001006].
[44] E. Abouzaid *et al.* [KTeV Collaboration], *Phys. Rev. D* **77**, 112004 (2008) [arXiv:0805.0031 [hep-ex]].
[45] T. Alexopoulos *et al.* [KTeV Collaboration], *Phys. Rev. D* **70**, 092006 (2004) [arXiv:hep-ex/0406002].
[46] B. Aubert *et al.* [BaBar Collaboration], *Phys. Rev. Lett.* **91**, 221802 (2003) [arXiv:hep-ex/0308042].
[47] J.-T. Wei *et al.* [Belle Collaboration], *Phys. Rev. Lett.* **103**, 171801 (2009) [arXiv:0904.0770 [hep-ex]].
[48] R. Aaij *et al.* [LHCb Collaboration], *J. High Energy Phys.* **1302**, 105 (2013) [arXiv:1209.4284 [hep-ex]].
[49] P.A.R. Ade *et al.* [Planck Collaboration], *Astron. Astrophys.* **594**, A13 (2016) [arXiv:1502.01589 [astro-ph.CO]].
[50] V.V. Anisimovsky *et al.* [E949 Collaboration], *Phys. Rev. Lett.* **93**, 031801 (2004) [arXiv:hep-ex/0403036].
[51] A.V. Artamonov *et al.* [E949 Collaboration], *Phys. Rev. Lett.* **101**, 191802 (2008) [arXiv:0808.2459 [hep-ex]].
[52] A.V. Artamonov *et al.* [BNL-E949 Collaboration], *Phys. Rev. D* **79**, 092004 (2009) [arXiv:0903.0030 [hep-ex]].
[53] A.V. Artamonov *et al.* [E949 Collaboration], *Phys. Rev. D* **72**, 091102 (2005) [arXiv:hep-ex/0506028].
[54] J.P. Lees *et al.* [BaBar Collaboration], *Phys. Rev. D* **87**, 112005 (2013) [arXiv:1303.7465 [hep-ex]].
[55] G. Anelli *et al.*, CERN-SPSC-2005-013, CERN-SPSC-P-326.
[56] T. Abe *et al.* [Belle II Collaboration], arXiv:1011.0352 [physics.ins-det].
[57] F. Bergsma *et al.* [CHARM Collaboration], *Phys. Lett. B* **157**, 458 (1985).
[58] S. Alekhin *et al.*, *Rep. Prog. Phys.* **79**, 124201 (2016) [arXiv:1504.04855 [hep-ph]].
[59] C. Adams *et al.* [LBNE Collaboration], arXiv:1307.7335 [hep-ex].
[60] G. Aad *et al.* [ATLAS Collaboration], arXiv:0901.0512 [hep-ex].
[61] G.L. Bayatian *et al.* [CMS Collaboration], *J. Phys. G* **34**, 995 (2007); S. Chatrchyan *et al.* [CMS Collaboration], *JINST* **3**, S08004 (2008).
[62] J.P. Chou, D. Curtin, H.J. Lubatti, *Phys. Lett. B* **767**, 29 (2017) [arXiv:1606.06298 [hep-ph]].